Polarization and Impedance Controlled Car

2024 IEEE AP-S Student Design Contest

Teo Bergkvist, Otto Edgren, Oscar Gren, Måns Jacobsson, and Christian Nelson
Lund University, Lund, Sweden

I. Introduction

As engineering students, we often learn about electromagnetic field theory from a theoretical perspective, which may render it hard to understand phenomena such as impedance and polarization. The Polarization and Impedance Controlled Car (PICC) provides a practical and engaging way to learn these principles using a radio-controlled car, a NanoVNA and on-body antennas. By manipulating wave polarization and impedance in real-time, users can see direct effects on the car's movement. This hands-on approach improves comprehension and makes classroom demonstrations more effective.

The PICC, shown in Fig. 1, is comprised of a pair of on-body antennas, a passive strip grid, a NanoVNA, a Raspberry Pi and a radio controlled car. In the following sections, we will detail how the

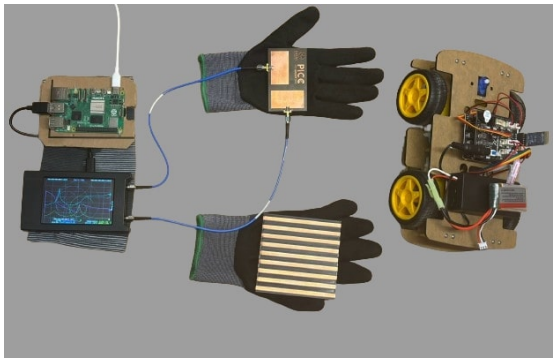

Fig. 1: The PICC

PICC functions, highlight its educational benefits, and explain the underlying principles of polarization and impedance which govern its operation. The project aims to bridge the gap between theoretical electromagnetics and its practical applications, providing a deeper insight into the physical phenomena and engineering challenges involved.

II. Background

Polarization indicates the orientation of the electric field — one common basis typically used in antenna application is linear polarization such as vertical and horizontal [1]. For the PICC a set of linearly polarized patch antennas are used, also commonly used by mobile phones and other electronics [2], together with a strip grid.

In an ideal scenario, when a wave impinges on a grid of parallel metal strips, the relative angle between the grid and the polarized wave dictates reflection intensity. Maximum reflection occurs when the grid is parallel to the wave's polarization, and minimal when they are orthogonal. The grid's orientation selectively reflects certain polarizations.

For this project, the changing impedance caused by bodies in the near field, such as the strip grid, is crucial to control the car. Near-field effects appear when working close to the antenna. Objects close by will couple to the antenna changing its impedance, particularly the other patch. To calculate the distance at which the far field starts one can use the Fraunhofer distance d_{F} [3], shown in (1). The parameter D stands for the largest dimension of the antenna which is the diagonal.

$$d_{\mathrm{F}} = \frac{2fD^2}{c} = \frac{2D^2}{\lambda} \tag{1}$$

The NanoVNA, is a compact and accessible form of a vector network analyzer (VNA), which measures two scattering parameters; S_{11} and S_{21}. They depend on the reference, load, input and source impedances Z_0, Z_L, Z_{IN} and Z_S respectively. Actual measurements are made by connecting to a matched load, $Z_L = Z_0$. The S_{11} parameter is known as the reflection coefficient which measures the portion of the signal sent from port 1 that is reflected back to port 1. The S_{21} parameter is the transmission coefficient measuring the portion of the signal from port 1 to port 2 [4].

In Fig. 2 it is shown how the S-parameters vary without external disruptions, with perfectly fabricated antennas and no connector losses depending on the angle between antenna and strip grid. When $\theta = 0°$ then the E-plane of the antenna is parallel

to the strip grid and if $\theta = 90°$ they are perpendicular [5].

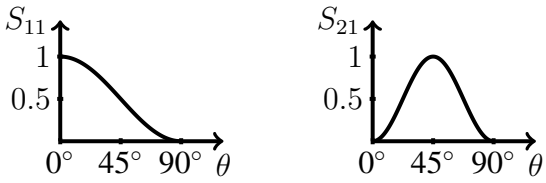

(a) S_{11} varying with θ (b) S_{21} varying with θ

Fig. 2: S_{11} and S_{21} varying ideally with the angle θ between antenna and strip grid. The $y-$axis is normalized and shows the reflected signal strength to each antenna.

In reality, other nearby bodies will affect the S-parameters by causing additional reflections and absorptions, varying the effective impedance values.

Various factors come into play when designing the antennas, such as the desired resonant frequency f, the speed of light c, the relative permittivity ε_{r} of the material and the height, h, of the dielectric material. The width, effective permittivity and length of the antenna can be calculated using (2), (3), and (4) respectively [6].

$$w = \frac{c}{f}\frac{1}{\sqrt{2(\varepsilon_{\mathrm{r}}+1)}} = \frac{\lambda}{\sqrt{2(\varepsilon_{\mathrm{r}}+1)}} \tag{2}$$

$$\varepsilon_{\mathrm{eff}} = \frac{\varepsilon_{\mathrm{r}}+1}{2} + \frac{\varepsilon_{\mathrm{r}}-1}{2}\cdot\left[\frac{1}{\sqrt{1+12(h/w)}}\right] \tag{3}$$

$$L = \frac{c}{2f\sqrt{\varepsilon_{\mathrm{eff}}}} - 2\Delta L = \frac{\lambda}{2\sqrt{\varepsilon_{\mathrm{eff}}}} - 2\Delta L \tag{4}$$

Due to fringing effects along the antenna edges – given $\varepsilon_{\mathrm{eff}}$, w and h – a small correction term ΔL is introduced in (4).

III. Physical Design and Specifications

The custom parts of the PICC consists of the patch antennas and the strip grid.

A. Antenna design

The antennas were designed to operate around $3.0\,\mathrm{GHz}$, a frequency that reduces overall design size due to its shorter wavelength. This ensures the antennas to be appropriately sized for on-body hand placement.

The patch antenna shown in Fig. 3a, is designed with two almost identical antennas propagating waves perpendicularly out of the plane. The left one sends out polarized waves oscillating in the y-direction. Waves from the right antenna oscillate in the x-direction. The substrate material is FR4 which has an approximate relative permittivity, ε_{r}, of 4.5 [7] at $3\,\mathrm{GHz}$. The thickness of the antenna patch is $1.6\,\mathrm{mm}$, where the thickness of the dielectric material is $1.53\,\mathrm{mm}$. Using (2), (3), and (4) the antenna dimensions were calculated to be $42.6\,\mathrm{mm}$ wide, $22.9\,\mathrm{mm}$ long. Finally, the length of the inset feed was experimentally chosen to be $2.8\,\mathrm{mm}$ from simulations to match the $50\,\Omega$ impedance from the connected cables. The Fraunhofer distance from (1) is calculated to be $184\,\mathrm{mm}$ indicating that the measurements used are in the near field region. Consequently near field effects will occur, which will alter the impedance, thus influencing the S-parameters.

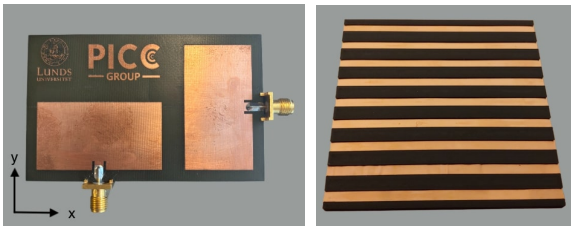

(a) Patch antenna (b) Strip grid

Fig. 3: (a) The patch antenna with two differently polarized antennas. (b) Strip grid made of copper and PLA plastic.

B. Strip grid

The strip grid, seen in Fig. 3b consist of two different materials, a 3D printed plate made out of PLA plastic with slots for $5\,\mathrm{mm}$ wide, $0.2\,\mathrm{mm}$ thick copper strips. The strip grid is made to reflect as much as possible of the chosen polarization and minimize the amount reflected of the orthogonal polarization. Strip grids of two different dimensions were tested, $200\,\mathrm{mm} \times 200\,\mathrm{mm}$ and $100\,\mathrm{mm} \times 100\,\mathrm{mm}$.

C. Final product

The PICC is shown in Fig. 1. The patch antenna and the strip grid are mounted on each hand. This enables fine adjustments of angles and distances, and is an engaging way to control the RC car. The pair of antennas are connected to the two ports on the NanoVNA. The NanoVNA is connected to the Raspberry Pi via USB-C. Finally, the Raspberry Pi sends control signals over bluetooth to the RC car.

All the components and materials including their prices can be viewed in Table I.

Table I: Bill of the materials using convertion rates 1 SEK = 0.093 USD and 1 EUR = 1.08 USD as of May 3rd 2024. The full list including links to all items can be found in our replication manual.

Items	Price	Source
RC car and controller	$73	Amazon
LiteVNA 64	$184	Amazon
Raspberry Pi 5	$78	Kjell & Co
Raspberry Pi 5 Power Adapter	$17	Electrokit
USB-A to USB-C cable	$17	Kjell & Co
2x 18650-batteries	$12	Electrokit
Gloves	$4	Biltema
Elbow sleeve	$9	Biltema
Micro SD card 64 GB	$30	Kjell & Co
Patch Antenna (PCB)	$20	PCBWay
SMA Connectors	$8	Amazon
Strip Grid Plate (3d-printed)	$11	IKDC Lund University
Flat Copper Wire	$13	Amazon
Hook-and-loop tape	$10	Biltema
Total:	$486	

IV. VNA Interaction

A key aspect of the PICC design was to facilitate interaction and data streaming from a NanoVNA to a computer. Many NanoVNA programs and python packages exist, however all are operated using a graphical user interface which is not desired for this project. Therefore as a part of this project, an effort was made to create a general-purpose python library called *pynanovna* [8]. It makes it possible to calibrate a NanoVNA, stream data continuously, plot data, save data, and more while being easy to incorporate into other projects. It is possible to download the open source package using pip. This is to our knowledge one of the first general-purpose python libraries that can stream data from a NanoVNA. *pynanovna* has been used for all NanoVNA-communication throughout the development of the PICC.

V. Measurement

To test the setup, the antenna was connected to the NanoVNA, calibrated before each measurement, and data was recorded using *pynanovna*. The S-parameters were measured with the strip grid at varying heights and angles. The strip grid was attached to a plastic arm attached to a stand of variable height, and the antenna was held in place by a temporary mount. A paper with angles drawn at $5°$ intervals between $0°$ to $90°$ were placed below the stand to measure angles. The antenna was kept still while the stand was moved to align with the drawn angles. The distance from the antenna was measured with a ruler from $20\,\mathrm{mm}$ to $100\,\mathrm{mm}$ with a $10\,\mathrm{mm}$ spacing.

VI. Simulation

We conducted simulations of the antenna and strip grid using *FEKO 2023* to provide a reference to compare to the measured results. A simplified strip grid was modelled using rectangular thin conductors. Only the smaller strip grid was modelled. The antenna was modelled assuming a $\varepsilon_\mathrm{r} = 4.5$ of the substrate and a dielectric loss tangent of $\tan\delta = 0.03$. All conductors were assumed perfect and thin. In Fig. 4a the simulation model is shown.

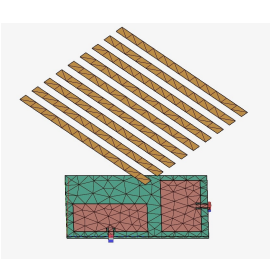

(a) Simulation mesh

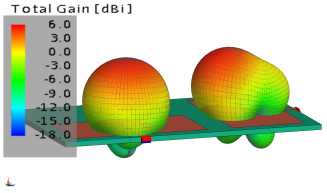

(b) Far field pattern for both patches. Total gain in decibels relative to isotropic.

Fig. 4: *FEKO* Simulations

VII. Antenna Performance

In Fig. 5, the difference between simulation and reality is shown for the base case with nothing in front of the antenna. In the simulation, the minimum reflectance of the antenna is $-55\,\mathrm{dB}$ at $2.88\,\mathrm{GHz}$ while in reality, it is $-45\,\mathrm{dB}$ at $2.97\,\mathrm{GHz}$. The bandwidth using a VSWR of 2:1 – i.e. when $S_{11} < -9.54\,\mathrm{dB}$ – is $156\,\mathrm{MHz}$ in the simulation and $177\,\mathrm{MHz}$ in reality. The shift in frequency is most likely due to the real-world permittivity of the substrate not matching the simulated value of $\varepsilon_\mathrm{r} = 4.5$. The change in magnitude could be caused by imperfections in fabrication, connector losses and reflections caused by surrounding objects. The 3D far field patterns in Fig. 4b shows that the antenna achieves a $6\,\mathrm{dB}$ power increase in the upwards direction compared to an isotropic antenna.

VIII. Signal Processing

The main part of the project was the processing of the input S-parameters to the output signals used for controlling speed and steering of the RC car.

A. Time-domain processing

To remove noise from signals reflected from objects other than the strip grid, a time-gating

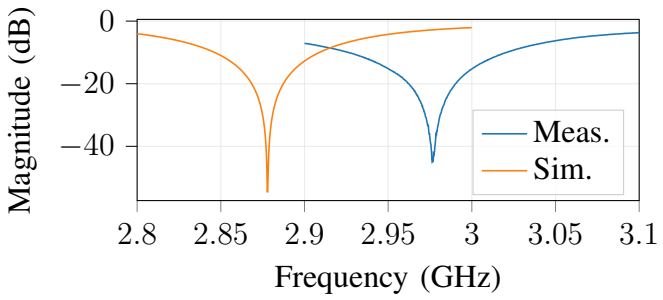

Fig. 5: S11 magnitude in the base case with nothing in front of the antenna. Meas. is the measurement of the real antenna Sim. is the simulation.

approach was used to isolate the relevant time response. Signals were zero-padded to a length of $n = 2^{14}$ for up-sampling and transformed to the time domain using the Inverse Fast Fourier Transform (IFFT). A Hanning Window was applied to isolate the highest peak, assumed to carry most of the strip grid position information. The signal was then transformed back to the frequency domain using FFT for further processing.

B. Frequency-domain processing

First, a reference sweep with no objects in front of the antenna is done, this reference sweep is denoted $S_{11,r}$ and $S_{21,r}$ respectively. This reference sweep is then subtracted from all future sweeps to obtain a difference in S_{11} and S_{21} from the reference position. At a specific height, the throttle should ideally be constant regardless of the angle of the strip grid. Using the theoretical behaviour, shown in Fig. 2, with $S_{11}(\theta) = \frac{\cos 2\theta + 1}{2}$ and $S_{21}(\theta) = \frac{1-\cos 4\theta}{2}$, the value of the expression $\sqrt{S_{11}(\theta)^2 + \frac{3}{4}S_{21}(\theta)^2}$ for the interval $0° \leq \theta \leq 45°$ is between 0.952 and 1.026. This expression served as a basis for the throttle function as it varies little with angle. The throttle function is computed as:

$$f = \sqrt{\overline{|S_{11} - S_{11,r}|}^2 + \alpha \overline{|S_{21} - S_{21,r}|}^2}, \quad (5)$$

where $\alpha \approx 9$ to compensate for the fact that S_{21} signal is much weaker than S_{11}. The amount of waves reflecting back to each antenna changes with the angle. At angle zero all the reflection from the strip grid is sent back to the same antenna, leading to a bigger S_{11} average and an extremely low S_{21} average. The proportion between these two parameters S_{21}/S_{11}, changes with the angle. It was found that taking the square root of S_{11} before calculating the proportion leads to a more stable angle measurement, thus the angle is calculated as:

$$\phi = \frac{\overline{|S_{21} - S_{21,r}|}}{\sqrt{\overline{|S_{11} - S_{11,r}|}}}. \quad (6)$$

These values are in an uncontrolled range and need to be restricted to the interval $[0, 1]$. A clamping function was used to clamp the values between their measured maximum and minimum:

$$\text{clamp}(x) = \begin{cases} 0, & x \leq x_{\min} \\ \dfrac{x - x_{\min}}{x_{\max} - x_{\min}}, & x_{\min} < x < x_{\max} \\ 1, & x \geq x_{\max} \end{cases},$$

where $x_{\min}$ and $x_{\max}$ are the measured minimum and maximum values.

IX. Signal Processing Performance

The signal processing was evaluated for both the $100\,\text{mm} \times 100\,\text{mm}$ and $200\,\text{mm} \times 200\,\text{mm}$ strip grid and compared with a simulation of the smaller. The graph in Fig. 6 shows the throttle computed from measured data according to (5) for different heights and angles. The differences in throttle between the angles is small at longer distances, but the throttle is substantially lower when the strip grid is at $30°$ and $45°$ at smaller distances. For the simulated grid the difference in throttle at different angles is very small. The graph in Fig. 7 shows the steering angle calculated from (6) at varying angles and a fixed $30\,\text{mm}$ distance.

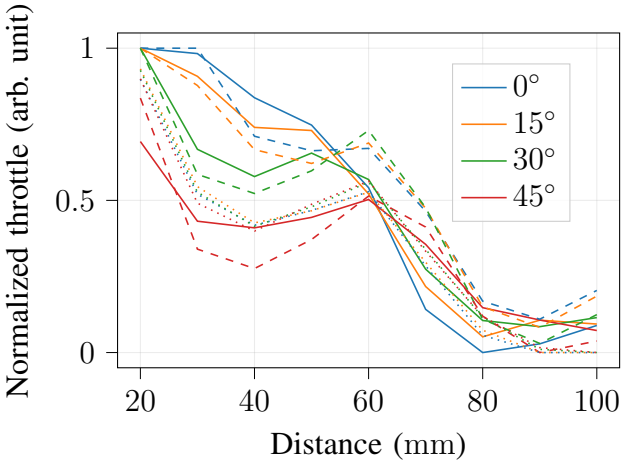

Fig. 6: Throttle for different distances and angles of the strip grid. $200\,\text{mm} \times 200\,\text{mm}$ strip grid is drawn dashed, $100\,\text{mm} \times 100\,\text{mm}$ solid, simulated data for $100\,\text{mm} \times 100\,\text{mm}$ strip grid is dotted.

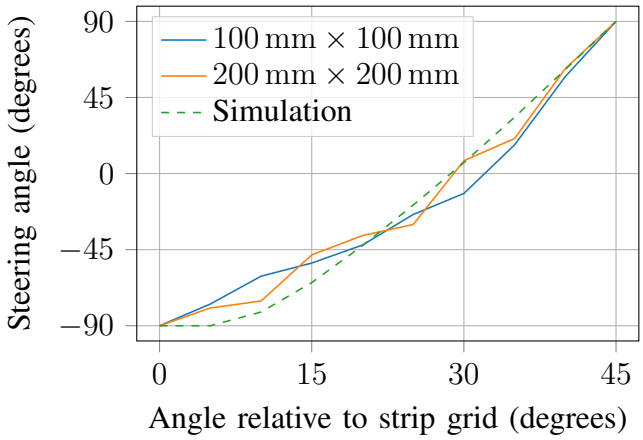

Fig. 7: Steering for different strip grid angles compared to simulation of $100\,\mathrm{mm} \times 100\,\mathrm{mm}$ strip grid at $30\,\mathrm{mm}$ distance.

X. Conclusion

The PICC offers a fun and intuitive way of learning the concepts of impedance and polarization. This project has shown that it is possible to generate speed and steering signals for an RC car by measuring impedance change in the near field, using a set of on-body antennas and a strip grid.

References

[1] D. J. Griffiths, *Introduction to Electrodynamics*. Pearson, 2013.

[2] "Circular and linear polarization of vsat antennas," Feb 2022, (Last visited 2023-12-20). [Online]. Available: https://www.linksystems-uk.com/circular-linear-polarization/

[3] M. N. Abdallah, T. K. Sarkar, M. Salazar-Palma, and V. Monebhurrun, "Where does the far field of an antenna start?" (Last visited 2024-05-16). [Online]. Available: https://ieeexplore.ieee.org/abstract/document/7590187

[4] S. J.Orfanidis, "S-parameters," (Last visited 2024-05-18). [Online]. Available: https://www.ece.rutgers.edu/~orfanidi/ewa/ch14.pdf

[5] C. A.Balanis, "Antenna theory," (Last visited 2024-05-18). [Online]. Available: https://ia800501.us.archive.org/30/items/AntennaTheoryAnalysisAndDesign3rdEd/Antenna%20Theory%20Analysis%20and%20Design%203rd%20ed.pdf

[6] H. Werfelli, K. Tayari, M. Chaoui, M. Lahiani, and H. Ghariani, "Design of rectangular microstrip patch antenna," (Last visited 2024-05-16). [Online]. Available: https://ieeexplore.ieee.org/abstract/document/7523197

[7] Mcl, "Fr4 material guide: What is fr4 material?" Apr 2024. [Online]. Available: https://www.mclpcb.com/blog/fr4-guide/

[8] P. group, "pynanovna," (Last visited 2024-05-17). [Online]. Available: https://pypi.org/project/pynanovna/

Teo Bergkvist is a third year undergraduate student in Engineering Mathematics. Teo has an interest in robotics, signal processing and software-defined radio. He has previously worked with research at Volvo Cars and with software development at Castle.

Oscar Gren is a third year undergraduate student in Engineering Mathematics at Lund University, with an interest in antenna simulations and machine learning.

Otto Edgren is a third year undergraduate student in Engineering Physics at Lund University looking to pursue a Master in Machine Intelligence.

Måns Jacobsson is a third-year Engineering Mathematics undergraduate at Lund University, with an interest in wireless communication and mathematical modeling for sustainability. He has previously worked with developing forecast and simulation models for green energy initiatives.

Christian Nelson received his M.Sc. degree in Engineering Physics from Lund University, Lund, Sweden in 2016. He is currently pursuing a Ph.D. in electrical engineering and wireless communication with the Department of Electrical Engineering and Information Technology, Lund University.